EXPERIMENTAL STUDY ON SCALING OF CIRCULAR TUBES SUBJECTED TO DYNAMIC AXIAL CRUSHING USING MODELS OF DIFFERENT MATERIALS

Leonardo M. Mazzariol[*]
Marcílio Alves
University of São Paulo - SP - Brazil
lmmazzariol@usp.br

Abstract. *The scaling of circular tubes axially impacted by a rigid mass is experimentally studied in the present work. As a mean to analyse similarity, scaled tubes (models or replicas) made of different material of the full-size structure (prototype) are used. Since the classical scaling laws does not provide the means to produce proper replicas for this case, a modification is made in these laws so that it is possible to take the difference in materials into account. However, despite the correction made to compensate for distortion effects, the results show that the models behave differently from the prototype, presenting lower reaction forces, lower capacity of absorbing energy, higher displacements, and different collapse modes. Furthermore, it is shown that material differences and scaling may affect the buckling mode and the fold length of the tubes.*

Keywords: *similarity, scaling, experimental, circular tube, impact*

1. INTRODUCTION

The understanding of a phenomenon starts from the observation of its nature. At first, one evaluates qualitatively which parameters have influence on the response of a specific set-up, then starts to modify their values to quantify cause-effect relations. By analyzing the response while varying the parameters it is possible to define dimensionless numbers (and dimensionless group), thus finding similar relations for different experiments. The Pi-Buckingham theorem states that structures having equal predominant dimensionless groups behave similarly, providing the basis for laws relating structures of different scales. This technique is called Similarity or Scaling Laws (Barenblatt, 2003).

It is well established in many investigations, such as (Booth *et al.*, 1983; Jiang *et al.*, 2006; Jones, 1997) that the direct application of "traditional" similarity laws on impact events may lead to unmatched results for model (scaled structure) representing prototype (full scale structure). One fact attributed to this behaviour is the non-scalability of strain rate effects, resulting in higher stresses in scaled models, stiffening their response in general. Oshiro and Alves (2009) presented a way to overcome these limitation by creating a different basis and distorting the scaling laws, modifying initial striker velocity to take strain rate effect into account. In addition, Mazzariol *et al.* (2011) stretched the formulation and imposed striker velocity arbitrarily, compensating energy in impact mass, allowing to overcome impact rig limitations.

Although many advances have been made on the modelling of impact events using models (Yulong *et al.*, 2008; Christoforou and Yigit, 2009; Snyman, 2010), the use of dissimilar materials is still a challenge. This possibility is of great interest since it allows to choose a different model construction method compared to prototype as well as may reduce costs involved due to material and impact rig limitations (Westine and Mullin, 1987; Cho *et al.*, 2005).

In the present investigation the response of an aluminium circular tube axially impacted is compared with models made of aluminum (scale $\beta = 1/2$) and mild steel ($\beta = 1/2$ and $\beta = 3/4$). The aluminium properties are quite different from the mild steel, so providing valuable means to analyse the scaling method. For this investigation, the main focus will be given to the similarity study. In what follows, Section 2 describes the similarity approach, while Section 3 depicts the experimental procedure. Section 4 discusses the obtained results and Section 5 encloses this article.

2. SIMILARITY

The technique in which a structure scaled by a factor β (model) is used to infer the real size structure (prototype) behaviour is termed similarity, scaling or similitude. This method has been extensively studied and widely applied in many fields (Barenblatt, 2003; Baker *et al.*, 1991). For impact phenomena, the main variables scaling factors are long known and summarized in Table 1. In order to achieve perfect similarity, the Π theorem asserts that all model predominant dimensionless numbers must be equal to the corresponding prototype dimensionless numbers,

$$(\Pi_i)_m = (\Pi_i)_p \tag{1}$$

with m and p referring to model and prototype, respectively.

Table 1: Factors relating the model variables to the prototype in *Mass-Length-Time* basis.

variable	factor	variable	factor
length, L	β	time, t	β
displacement, δ	β	velocity, V	1
mass, G	β^3	strain rate, $\dot{\varepsilon}$	$1/\beta$
strain, ε	1	acceleration, A	$1/\beta$
stress, σ	1	energy, E'	β^3
force, F	β^2		

As mentioned, structures under severe dynamic loads usually do not follow scaling laws due to effects such as material strain rate sensitivity, material failure, thermal response, gravity etc. When a single geometric scaling factor is not capable of relating a prototype and a model, it is necessary to define other scaling factors, an approach called distorted similarity. From that approach Oshiro and Alves (2004) defined a distortion in velocity factor

$$\beta_{V_0} = \sqrt{\frac{\sigma_{d_m}}{\sigma_{d_p}}} = \sqrt{\frac{f(\beta_{V_0}\, \dot{\varepsilon}_m^{nc})}{f(\beta\, \dot{\varepsilon}_m^{nc})}} \tag{2}$$

in terms of β, the length scaling factor; σ_d, dynamic stress, which is represented here as a function f of initial condition, V_0, β and structural response, $\dot{\varepsilon}$ and, finally, as function of non-corrected or scaled strain rate $\dot{\varepsilon}_m^{nc} = \dot{\varepsilon}_p/\beta$. Impact mass is scaled according to $\beta_G = \beta^3$. Equation 2 does not specify a viscoplastic relation to be used, however the authors used the Cowper-Symonds equation (Jones, 1997)

$$\frac{\sigma_d}{\sigma_0} = 1 + \left(\frac{\dot{\varepsilon}}{D}\right)^{1/p}, \tag{3}$$

being σ_0, reference flow stress; p and D, viscoplastic material properties. As it can be seen from Eq. 2, the uncorrected model strain-rate value is needed to define the distorted β_{V_0}, which was calculated using analytical formulation.

Following the same approach, Oshiro and Alves (2009) wrote Eq. 2 in terms of the Norton equation (Lemaitre and Chaboche, 1991) for the viscoplastic behaviour, $\sigma_d = \sigma_0\, (\dot{\varepsilon}/\dot{\varepsilon}_0)^q$, resulting

$$\beta_V = \beta^{q/(q-2)} \tag{4}$$

also defining impact mass factor $\beta_G = \beta^3$, for model and prototype made of same material. Equation 4 has advantage over Eq. 2 since calculated β_V does not depend on structural response, $\dot{\varepsilon}$. By following these lines, Mazzariol *et al.* (2010) modified the impact mass as $\beta_G = \beta^{3-q}$ to obtain corrected model for $\beta_V = 1$.

Closer to the present study, Alves and Oshiro (2006) uses a variation of Eq. 2, describing the behaviour of model and prototype made of different material, using aluminium as model (low sensitivity to strain rate) and steel as prototype,

$$\beta_V = \sqrt{\frac{\sigma_{0m}}{\sigma_{0p}\left[1 + \left(\frac{\dot{\varepsilon}_p}{D}\right)^{1/p}\right]}}, \tag{5}$$

where p, D, σ_{0_m},σ_{0_p} are material parameters for Cowper-Symonds equation. As it can be seen, the velocity correction depends on structural response $\dot{\varepsilon}_p$ that must be obtained numerically or theoretically.

As means to calculate the velocity factor, the present study used the dimensionless numbers obtained in Oshiro and Alves (2009)

$$\Pi_1 = \left[\frac{A^3 G}{V_0^4 \sigma_d}\right], \ \Pi_2 = \left[\frac{t^3 \sigma_d V_0}{G}\right], \ \Pi_3 = \left[\frac{\delta^3 \sigma_d}{G V_0^2}\right], \ \Pi_4 = \left[\frac{\dot{\varepsilon} G^{1/3}}{(\sigma_d V_0)^{1/3}}\right] \quad \text{and} \quad \Pi_5 = \left[\frac{\sigma}{\sigma_d}\right], \tag{6}$$

which were written in VSG basis (initial velocity, V_0, dynamic stress, σ_d, and impact mass, G) instead of commonly used *Mass-Length-Time*. Rearranging Π_3, one obtains

$$(\Pi_3)_m = (\Pi_3)_p \; \rightarrow \; \left[\frac{\delta_m^3 \sigma_{dm}}{G_m V_{0m}^2} \right] = \left[\frac{\delta_p^3 \sigma_{dp}}{G_p V_{0p}^2} \right] \; \rightarrow \; \left(\frac{\delta_m}{\delta_p} \right)^3 \cdot \left(\frac{\sigma_{dm}}{\sigma_{dp}} \right) \cdot \left(\frac{G_p}{G_m} \right) \cdot \left(\frac{V_{0p}}{V_{0m}} \right)^2 = 1 \,. \tag{7}$$

Defining $\beta_G = G_m/G_p$, impact mass G ratio between model and prototype, $\beta_V = V_{0m}/V_{0p}$, the velocity factor, dynamic stress factor $\beta_\sigma = \sigma_{d_m}/\sigma_{d_p}$ and considering that model has the same deformation pattern as prototype, $\beta = \delta_m/\delta_p$, Eq. 7 can be rewritten as

$$(\beta)^3 \cdot (\beta_\sigma) \cdot \left(\frac{1}{\beta_G} \right) \cdot \left(\frac{1}{\beta_V} \right)^2 = 1 \; \rightarrow \; \frac{\beta^3 \beta_\sigma}{\beta_G \beta_V^2} = 1 \; \rightarrow \; \beta_G = \frac{\beta^3 \beta_\sigma}{\beta_V^2} \tag{8}$$

Similarly, velocity scaling factor can also be calculated

$$\beta_V = \sqrt{\frac{\beta^3 \beta_\sigma}{\beta_G}} \,. \tag{9}$$

Rearranging Π_4,

$$(\Pi_4)_m = (\Pi_4)_p \; \rightarrow \; \left[\frac{\dot{\varepsilon}_m G_m^{\frac{1}{3}}}{(\sigma_{d_m} V_{0_m})^{\frac{1}{3}}} \right] = \left[\frac{\dot{\varepsilon}_p G_p^{\frac{1}{3}}}{(\sigma_{d_p} V_{0_p})^{\frac{1}{3}}} \right] \; \rightarrow \; \left(\frac{\dot{\varepsilon}_m}{\dot{\varepsilon}_p} \right) \cdot \left(\frac{G_m}{G_p} \right)^{\frac{1}{3}} \cdot \left(\frac{\sigma_{d_p}}{\sigma_{d_m}} \right)^{\frac{1}{3}} \cdot \left(\frac{V_{0_p}}{V_{0_m}} \right)^{\frac{1}{3}} = 1 \,,$$

condensing in terms of β_G, β_V, β_σ and writing the strain-rate scaling factor $\beta_{\dot{\varepsilon}} = \dot{\varepsilon}_m/\dot{\varepsilon}_p$,

$$(\beta_{\dot{\varepsilon}}) \cdot (\beta_G)^{1/3} \cdot \left(\frac{1}{\beta_\sigma} \right)^{1/3} \cdot \left(\frac{1}{\beta_V} \right)^{1/3} = 1 \; \rightarrow \; \beta_{\dot{\varepsilon}} \left(\frac{\beta_G}{\beta_\sigma \beta_V} \right)^{1/3} = 1 \; \rightarrow \; \beta_{\dot{\varepsilon}} = \left(\frac{\beta_\sigma \beta_V}{\beta_G} \right)^{1/3} \,. \tag{10}$$

Inserting Eq. 8 in Eq. 10 results in

$$\beta_{\dot{\varepsilon}} = \frac{\beta_V}{\beta} \,, \tag{11}$$

As mentioned, it is assumed that $\sigma_d = \sigma_d(\dot{\varepsilon} \ldots)$. Then, to solve Eq. 8 or 9 one must write the dynamic stress σ_d using a viscoplastic formulation (Norton or Cowper-Symonds, for instance) and consequently obtain the dynamic scaling factor β_σ. By inserting Cowper-Symonds, Eq. 3 into β_σ it is generated

$$\beta_\sigma = \frac{\sigma_{0_m} \left[1 + (\dot{\varepsilon}_m/D_m)^{1/p_m} \right]}{\sigma_{0_p} \left[1 + (\dot{\varepsilon}_p/D_p)^{1/p_p} \right]} \,. \tag{12}$$

Inserting $\dot{\varepsilon}_m = \beta_{\dot{\varepsilon}} \dot{\varepsilon}_p$, and $\beta_{\dot{\varepsilon}} = \beta_V/\beta$ in Eq. 12, one obtains

$$\beta_\sigma = \frac{\sigma_{0_m} \left[1 + (\beta_V \dot{\varepsilon}_p/\beta D_m)^{1/p_m} \right]}{\sigma_{0_p} \left[1 + (\dot{\varepsilon}_p/D_p)^{1/p_p} \right]} \tag{13}$$

that also depends on $\dot{\varepsilon}_p$ and Cowper-Symonds material properties. Both Eq. 13 when used in Eq. 9 while taking $\beta_{\sigma_0} = \sigma_{0_m}/\sigma_{0_m}$ results in the velocity scaling factor:

$$\beta_V = \sqrt{\frac{\beta^3 \beta_{\sigma_0}}{\beta_G} \frac{\left[1 + (\beta_V \dot{\varepsilon}_p/\beta D_m)^{1/p_m} \right]}{\left[1 + (\dot{\varepsilon}_p/D_p)^{1/p_p} \right]}} \,, \tag{14}$$

that considers strain-rate effect and different materials. Scaling factors for acceleration β_A and time, β_t, are obtained by inserting Eq. 9 in dimensionless numbers Π_1 and Π_2:

$$\Pi_1 = \left[\frac{A^3 G}{\sigma_d V_0^4}\right] \quad \rightarrow \quad \frac{\beta_A^3 \beta_G}{\beta_{\sigma_d}\beta_V^4} = 1 \quad \rightarrow \quad \beta_A = \frac{\beta_V^2}{\beta}, \tag{15}$$

$$\Pi_2 = \left[\frac{t^3 \sigma_d V_0}{G}\right] \quad \rightarrow \quad \frac{\beta_t^3 \beta_{\sigma_d}\beta_V}{\beta_G} = 1 \quad \rightarrow \quad \beta_t = \frac{\beta}{\beta_V}. \tag{16}$$

Naturally, force factor, β_F, comes from Newton's law

$$\beta_F = \beta_G\,\beta_A\,, \tag{17}$$

and energy factor, from dimensional analysis,

$$\beta_E = \beta_F\beta\,. \tag{18}$$

Note that β_V, Eq. 13, is a recursive function. Moreover, this approach relays on structural response. In the present work, Cowper-Symonds constitutive equation was chosen because it represents the aluminium and mild steel behaviour better than Norton equation does.

3. EXPERIMENTAL PROCEDURE

3.1 MATERIAL PROPERTIES

Material characterization plays an important role when applying similarity laws to represent impact events. Both quasi-static and viscoplastic behaviour are needed to calculate the initial conditions for experiments in models and hence infer the prototype comportment. As can be imagined, it is frequently not possible to relate two different material quasi-static curves using only a scalar. The same difficulty may be easy to observe in viscoplastic behaviour, resulting in scaling factors as function of structural response. Although the desire is to find the exact solution, one should be inclined toward an approximation instead of an absence of solution.

The structure chosen as prototype is a circular shell made of aluminium with a external diameter $d = 50.8\,\text{mm}$, thickness $t = 2\,\text{mm}$ and length $L = 150\,\text{mm}$. The models have two scales, $\beta = 0.5$ ($d = 25.4$, $t = 1.0\,\text{mm}$ and $L = 75\,\text{mm}$) made of aluminium and steel, and $\beta = 0.75$ made of steel ($d = 38.1$ $t = 1.5$ and $L = 112.5\,\text{mm}$). Ring specimens with height $H' = 2t$ were obtained from the shells and tested under quasi-static compression using a universal testing machine. The calculated average stress – plastic strain curves are shown in Fig. 1. In addition, the quasi-static curves from model material were scaled according to each reference stress factor β_{σ_0} and referred as "corrected". Since the structural response in terms of deformation is not known, the yield stress was used as reference stress, i.e., $\beta_{\sigma_0} = \sigma_{Y_m}/\sigma_{Y_p}$, so as to not over- or underestimate the model response by assuming a specific average strain value, which led to a proper representation.

Table 2: Material properties for prototype and models.

	β	Density	Young Modulus	Mean Yield Stress σ_Y	β_{σ_0}	$D^{(1)}$	$p^{(1)}$
	[–]	[10^3 kg/m^3]	[GPa]	[MPa]	[–]	[1/s]	[–]
Aluminium (Prototype)	1:1	2.71	70	161.2	—	6500	4
Aluminium (Model)	1:2	2.71	70	249.9	1.55	6500	4
Steel 1 (Model)	3:4	7.85	210	308.6	1.91	40.4	5
Steel 2 (Model)	1:2	7.85	210	420.5	2.61	40.4	5

[(1)] viscoplastic properties are assumed to be classical aluminium and mild steel, obtained from Jones (1997)

The viscoplastic behaviour is described as function of Cowper-Symonds equation, while the parameters are by assumption the found in literature (Jones, 1997), $p_{alu} = 4$ and $D_{alu} = 6500/\text{s}$ for aluminium, $p_{steel} = 5$ and $D_{steel} = 40.4/\text{s}$ for steel models. The material information needed to calculate initial conditions are shown in Table 2.
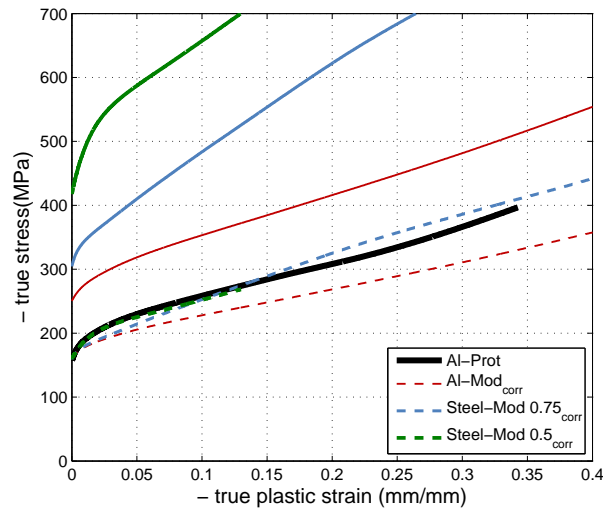
Figure 1: Quasi-static mechanical properties for prototype and models materials. Solid lines represent material averaged curves obtained in ring compression tests and dashed lines shows these curves divided by β_{σ_0}, i.e., "scaled quasi-static curves". Although β_{σ_0} is calculated using the 0.2% yield stress criterium, the models plastic curves are well represented by using only a scalar.

3.2 INITIAL CONDITIONS

The prototype is aimed to be impacted with a plane striker with a mass of $G = 300$ kg at a initial velocity of $V_0 = 4.5$m/s. These conditions were defined as a mean to generate axisymmetric progressive buckling of the prototype tube. For this deformation pattern, the structural response in terms of strain rate, $\dot{\varepsilon}$, is given approximately for a simplified model by Jones (1997):

$$\dot{\varepsilon} = \frac{V_{\text{avg}}}{4R}, \tag{19}$$

where V_{avg} stands for average velocity for a single fold and R, the tube radius. Assuming a constant reaction force for all folds, the average velocity can be written as $V_{\text{avg}} = 0.5\,V_0$. Thus applying to Eq. 19 for prototype conditions ($R = 50.8/2$ mm and $V_0 = 4500$ mm/s),

$$\dot{\varepsilon}_{\text{avg}} = \dot{\varepsilon}_p = \frac{4500/2}{4R} = 22.1/\text{s}, \tag{20}$$

one obtain the average structural response for prototype, $\dot{\varepsilon}_p$.

As can be observed in Eq. 14, to calculate β_V one must first define a β_G value. The prototype impact mass was defined as 287 kg, as close as possible to 300 kg. The model impact mass values were chosen based on the drop weight masses available for the experiments and keeping $V_0 < 8$ m/s, a setup limitation. For instance, for steel model $\beta = 0.5$, two different values were chosen: $G_m = 56.5$ kg (referred as High Speed - HS) and $G_m = 118$ kg (Low Speed - LS). The corrected initial conditions for all experiments are summarised in Tab. 3.
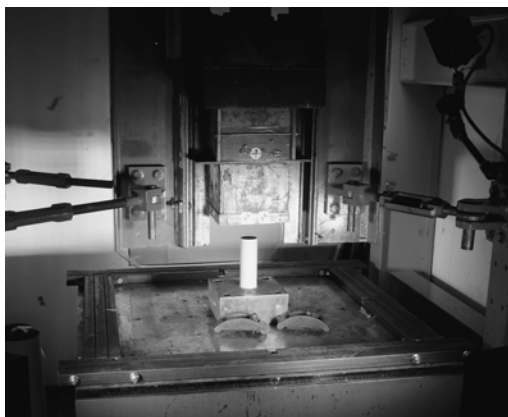
3.3 EXPERIMENTS

The tubes were cut under a tolerance of 0.1 mm from the same longer tube for each material. In addition, the faces were finished by sanding so as to obtain a plain and smooth top and bottom surfaces while keeping sharp edges. The tubes were freely positioned at the drop hammer, Fig. 2a, while the mass was raised to a specific height and dropped, deforming the tube, Fig. 2b. Initial conditions of the experiments are listed in Tab. 3. Velocity was measured using a Laser Vibrometer (Polytec OFV3020/323) aimed on top of impact mass and acquired using a National Instruments (BNC2111) at 100kHz.

The beginning of compression phase was taken as the maximum negative measured velocity and the end of test was defined as the maximum positive velocity. Displacement and acceleration at the top of the tube were obtained by integrating and differentiating the velocity data, respectively. Acceleration is then multiplied by mass to evaluate instantaneous force, which was filtered using moving average. If we assume that all energy lost of the drop mass was dissipated as deformation of the tube, one has

Table 3: Initial conditions for prototype and corrected velocity and mass for models.

	β [–]	Impact Mass, G [Kg]	β_V	Velocity, V_0 [m/s]
Aluminium (Prototype)	1:1	287	—	4.50
Aluminium (Model)	1:2	56.5	1.01	4.55
Steel 1 (Model)	3:4	232	1.26	5.69
Steel 2 (Model) HS	1:2	56.5	1.69	7.59
Steel 2 (Model) LS	1:2	118	1.14	5.14

(a) Test setup.

(b) Prototype after test.

Figure 2: Experimental setup.

$$E = \int_0^{\delta_{\max}} F \, d\delta, \tag{21}$$

where $F = G A$ is the instantaneous force; G, impact mass; A the acceleration and $\delta_{\max}$ is the maximum displacement. To compare models and prototype, the representative displacement of each scaled model was taken as the mean value of the tested replicas. The same was made for force values.

In order to directly compare models response to the prototype behaviour, it is necessary to apply the corresponding scaling factors for displacement, δ, time (Eq. 16), force (Eq. 17), and energy (Eq. 18). Figure 3a shows the displacement at the top of the tube as a function of time. It can be seen a significant divergence in the models when they are compared to the prototype. Furthermore, it is noticed a general softening of replicas behaviour. In Fig. 3b the maximum displacement in all experiments are compared to the expected curve (generated by using the prototype as reference and applying the scaling factors).

The reaction force versus displacement at the top of the tube is shown in Fig. 4a. As a mean to visualize the curves tendency, a stronger filter for the data was applied, resulting in Fig. 4b. It can be seen a rather significant difference in models response; they presented lower values of force and higher displacements in comparison to the prototype. In these tests, the $\beta = 1/2$ aluminium model (dark blue dashed curve) generated the closest response to the prototype (black continuous curve). Also, both $\beta = 1/2$ steel models behaved likewise even with different combinations of impact velocity and mass. In all cases the peak force took place when the scaled displacement reached about 5 mm. As it will be seen later, the prototype curve is compatible with the six folds formed during the impact event. The same behaviour is difficult to observe in models owing to equipment restrictions.

Maximum displacement and average force are summarised in Tab. 4. For the tested cases, both average force and displacement have low values of dispersion. It can be seen that average force is lower on models (21% lower in steel models and 12% for aluminium) resulting in larger displacements to absorb the same amount of energy. The higher values of displacement is due to the less energy absorbed by length in diamond buckling mode (Abramowicz and Jones, 1984) in comparison to concertina (or axisymmetric) buckling mode obtained in the prototype. This feature can be substantiated by the energy versus displacement curve (Fig. 5) in which the lower capacity of absorbing energy of the models are clear. These features are discussed later when the experimented tubes collapse modes are compared. Finally, the absorbed
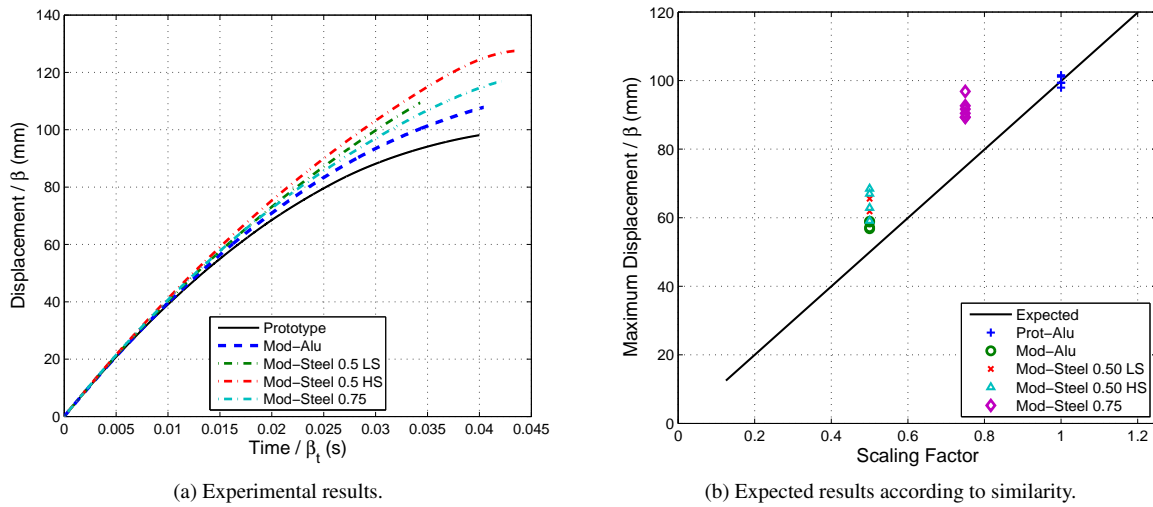
(a) Experimental results.

(b) Expected results according to similarity.

Figure 3: Experimental correlation for Displacement between model results and prototype.
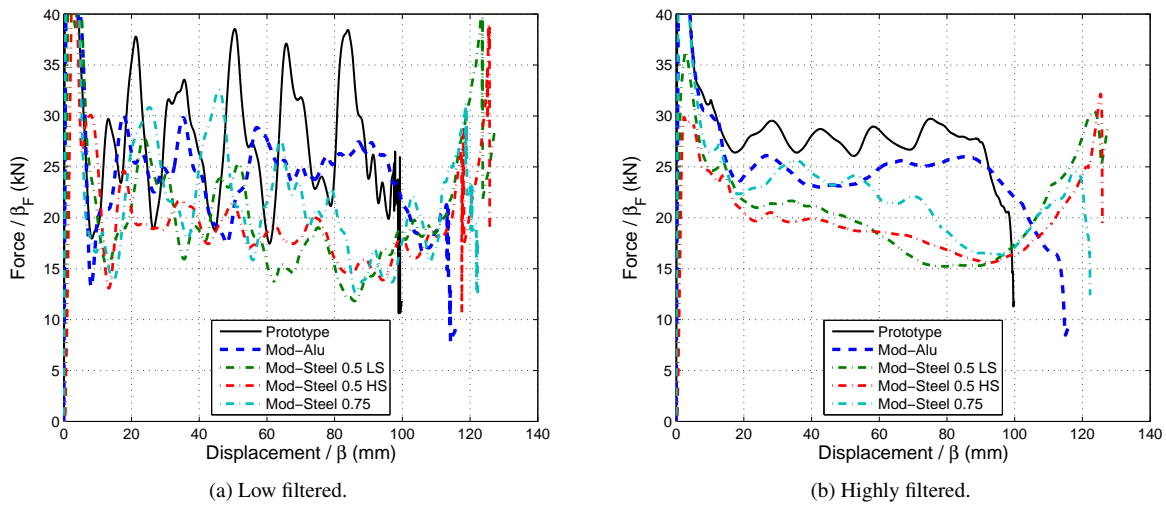

(a) Low filtered.

(b) Highly filtered.

Figure 4: Experimental correlation for Force between model results and prototype.

energy shows what can be seen on average force results from Tab. 4, a less stiff model requires more displacement to absorb the same energy. In addition, steel models ($\beta = 0.5$) were not able to deform enough to absorb the same energy, limited by the effective deformable length.

Table 4: Average results for prototype and models.

	Average Force[(1)] F_{avg}	F_{avg}/β_F	Difference	Maximum Displacement δ_{max}/β	Difference
	[kN]	[kN]	[%]	[mm]	[%]
Aluminium (Prototype)	28.52 ± 0.28	—	—	99.86 ± 1.48	—
Aluminium (Model)	10.01 ± 0.13	24.92 ± 0.31	-12.26	115.8 ± 2.22	15.96
Steel 1 (Model)	39.97 ± 2.19	23.23 ± 1.28	-18.54	122.3 ± 3.78	22.47
Steel 2 (Model) - HS	23.26 ± 0.99	22.58 ± 1.66	-24.09	128.7 ± 8.46	28.88
Steel 2 (Model) - LS	25.26 ± 1.85	21.65 ± 0.93	-20.82	127.4 ± 5.21	27.58

[(1)] Average force was calculated as mean of the $\int F \mathrm{d}\delta / \delta_{max}$ for each test.

L. M. Mazzariol and M. Alves
Experimental Study on Scaling of Circular Tubes Subject to Dynamic Axial Crushing Using Models of Different Materials
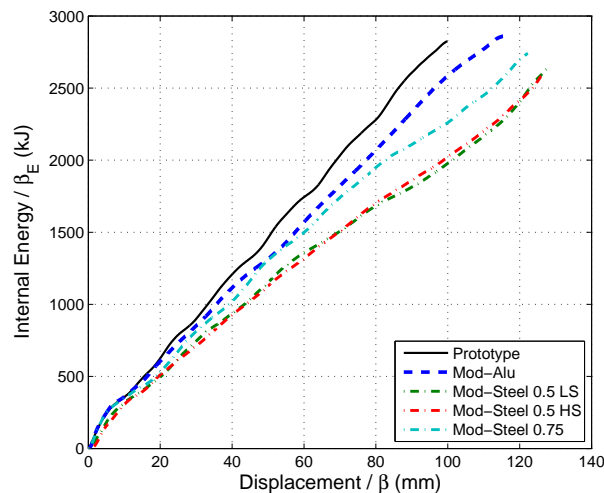

Figure 5: Experimental correlation for Energy between model results and prototype.

4. DISCUSSIONS

Quasi-static and dynamic material properties differs significantly between models and prototype, Tab. 2. For instance, quasi-static stress factor, β_{σ_0}, ranges from 1.55 (aluminium model) to 2.61 (steel model $\beta = 0.5$). These materials were purposely chosen so that an analysis of different materials effect could be made.

As earlier observed, the model presented rather different results from the prototype, Figs. 3 to 5. These discrepancies in force and displacement can be attributed to the different buckling modes produced in the tests, Figs. 6 to 10. It is known that concertina mode (axisymmetric) absorbs more energy per unit length if compared to diamond pattern (Abramowicz and Jones, 1984). *A priori* a comparison between model and prototype tubes response is inaccurate due to differences in the collapse mode. This is explained by the fact that different geometry configurations are not similar and therefore cannot be directly compared (Baker *et al.*, 1991).

For axisymmetric collapse mode, another important issue was found during the tests. The theoretical fold length for this case is given by $l = (\pi R H/\sqrt{3})^{1/2}$ (Abramowicz and Jones, 1986; Jones, 1997), being R and H the tube radius and thickness, respectively, that results in $l = 9.60$ mm for prototype, and $l = 4.80$ mm for model $\beta = 0.5$. Therefore, l is dependant of geometry but not material. It should lead to model and prototype similar fold lengths even when the material is different. However, as it can be seen in Fig.10, they are not proportional since the model used the entire length to develop 6 hinges ($l = 4.92$ mm, approximately) whereas the prototype still have an undeformed length at the superior portion ($l = 16.67$ mm, approximately). In conclusion, the equation that describes l is missing information regarding material and scaling effect.

5. CONCLUSIONS

This paper presented a study on scaling of circular tubes made of different materials. A set of aluminium tubes with diameter of 50.8mm, thickness of 2mm and 150mm height was impacted by a mass of 287 kg at 4.5 m/s and used as reference (prototype) while three different tubes were used as models (aluminium and steel in half-scale and steel in three-fourths scale). The differences in material quasi-static properties were taken into account by changing impact mass according to a formulation presented in Section 2, while the increase in dynamic stress due to strain-rate was considered by changing impact velocity. Despite of following the distorted equations, models showed to be less resistant and allowed a larger displacement if compared to prototype, a fact attributed to diamond buckling mode that absorbs less energy per unit of length. Even though comparing different buckling modes the average force error was less than -25% with displacement error of 20% which can be deemed as a good result. Finally, further investigation on fold length may allow researchers to obtain similar global deformation pattern for axially impact circular tubes using model and assuring that material quasi-static and viscoplastic behaviour are taken into account.

6. ACKNOWLEDGMENTS

Figure 6: Prototype made of aluminium. Samples 1-5 from left to right. All except sample #3 buckled as concertina or axisymmetric mode. Concertina mode developed 6 folds and left enough length for a seventh.

Figure 7: Aluminium models ($\beta = 0.5$) buckled as diamond mode. The initial compression phase results in two folds in concertina mode, followed by unstable diamond folds.

Figure 8: Steel models ($\beta = 0.75$). All 7 tubes buckled as diamond mode. The last, #7, reach the maximum of 3 concertina folds.
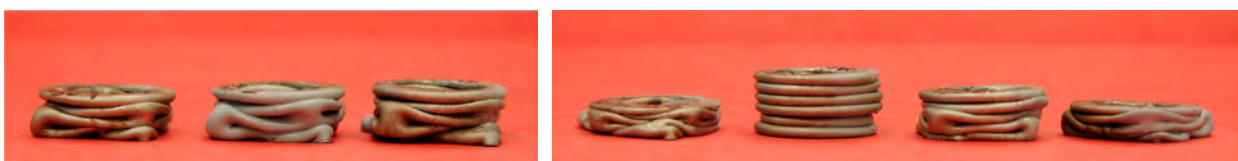
(a) Low Speed.

(b) High Speed. Only one model buckled as concertina mode. In addition, a full buckled concertina mode spent all tube length to develop 6 folds.

Figure 9: Steel models ($\beta = 0.50$). Low and High speed initial conditions were due to impact rig limitations on available mass. Only one of these seven tubes buckled as concertina, while other developed diamond modes.

Figure 10: Prototype made of aluminium developed shorter folds than model made of steel ($\beta = 0.50$). It was expected a similar global aspect since fold length is usually defined as function of geometrical parameters only (Jones, 1997).

7. REFERENCES

Abramowicz, W. and Jones, N., 1986. "Dynamic progressive buckling of circular and square tubes". *International Journal of Impact Engineering*, Vol. 4, No. 4, pp. 243 – 270. ISSN 0734-743X.

Abramowicz, W. and Jones, N., 1984. "Dynamic axial crushing of circular tubes". *International Journal of Impact Engineering*, Vol. 2, No. 3, pp. 263 – 281. ISSN 0734-743X.

Alves, M. and Oshiro, R.E., 2006. "Scaling the impact of a mass on a structure". *International Journal of Impact Engineering*, Vol. 32, No. 7, pp. 1158 – 1173. ISSN 0734-743X.

Baker, W.E., Westine, P.S. and Dodge, F.T., 1991. *Similarity Methods in Engineering Dynamics: Theory and Practice of Scale Modeling*. Elsevier Science Publishers, Amsterdam, 1st edition.

Barenblatt, G., 2003. *Scaling*. Cambridge Texts in Applied Mathematics. Cambridge University Press. ISBN 9780521533942.

Booth, E., Collier, D. and Miles, J., 1983. "Impact scalability of plated steel structures". In N. Jones and T. Wierzbicki, eds., *Structural Crashworthiness*, Butterworths & Co. Publishers, London, pp. 136–174.

Cho, U., Dutson, A.J., Wood, K.L. and Crawford, R.H., 2005. "An advanced method to correlate scale models with distorted configurations". *J Mech Des*, Vol. 127, No. 1, pp. 78–85. ISSN 1050-0472.

Christoforou, A.P. and Yigit, A.S., 2009. "Scaling of low-velocity impact response in composite structures". *Composite Structures*, Vol. 91, No. 3, pp. 358 – 365. ISSN 0263-8223.

Jiang, P., Wang, W. and Zhang, G., 2006. "Size effects in the axial tearing of circular tubes during quasi-static and impact loadings". *International Journal of Impact Engineering*, Vol. 32, No. 12, pp. 2048 – 2065. ISSN 0734-743X.

Jones, N., 1997. *Structural Impact*. Cambridge University Press, New York, USA, 1st edition.

Lemaitre, J. and Chaboche, J.L., 1991. *Mechanics of solids materials*. Cambridge University Press, Cambridge, 1st edition.

Mazzariol, L.M., Oshiro, R.E., Calle, M.A.G. and Alves, M., 2010. "Scaling of stiffened panels subjected to impact load". In E.N. Dvorkin and M.B. Goldschmidt, eds., *MECOM-CILAMCE*. AMCA, Buenos Aires, pp. 1275–1289.

Mazzariol, L.M., Oshiro, R.E., Calle, M.A.G., Moura, R.T. and Alves, M., 2011. "Evaluating velocity and mass correction on scaling of structures subjected to impact loading". In E. Fancello, P. de TarÇo, R. MendonÇa and M. Alves, eds., *Proceedings of the International Symposium on Solid Mechanics. Florianopolis*. ABCM, Florianopolis, SC, Brazil, pp. 353–366.

Oshiro, R.E. and Alves, M., 2004. "Scaling impacted structures". *Archive of Applied Mechanics*, Vol. 74, pp. 130–145. ISSN 0939-1533.

Oshiro, R. and Alves, M., 2009. "Scaling of structures subject to impact loads when using a power law constitutive equation". *International Journal of Solids and Structures*, Vol. 46, No. 18-19, pp. 3412–3421. ISSN 0020-7683.

Snyman, I., 2010. "Impulsive loading events and similarity scaling". *Engineering Structures*, Vol. 32, No. 3, pp. 886 – 896. ISSN 0141-0296.

Westine, P.S. and Mullin, S.A., 1987. "Scale modeling of hypervelocity impact". *International Journal of Impact Engineering*, Vol. 5, No. 1Ű4, pp. 693 – 701. ISSN 0734-743X. <ce:title>Hypervelocity Impact Proceedings of the 1986 Symposium</ce:title>.

Yulong, L., Yongkang, Z. and Pu, X., 2008. "Study of similarity law for bird impact on structure". *Chinese Journal of Aeronautics*, Vol. 21, No. 6, pp. 512 – 517. ISSN 1000-9361.

8. RESPONSIBILITY NOTICE

The authors are the only responsible for the printed material included in this paper.